

Alloying effects on the optical properties of $\text{Ge}_{1-x}\text{Si}_x$ nanocrystals from TDDFT and comparison with effective-medium theory

Silvana Botti,^{1,2,3} Hans-Christian Weissker,^{1,3} and Miguel A. L. Marques^{2,3}

¹*Laboratoire des Solides Irradiés, École Polytechnique, CNRS, and CEA-DSM, F-91128, Palaiseau, France*

²*Laboratoire de Physique de la Matière Condensée et Nanostructures, Université Lyon I and CNRS, F-69622 Villeurbanne Cedex, France*

³*European Theoretical Spectroscopy Facility (ETSF)*

(Dated: October 26, 2018)

We present the optical spectra of $\text{Ge}_{1-x}\text{Si}_x$ alloy nanocrystals calculated with time-dependent density-functional theory in the adiabatic local-density approximation (TDLDA). The spectra change smoothly as a function of the composition x . On the Ge side of the composition range, the lowest excitations at the absorption edge are almost pure Kohn-Sham independent-particle HOMO-LUMO transitions, while for higher Si contents strong mixing of transitions is found. Within TDLDA the first peak is slightly higher in energy than in earlier independent-particle calculations. However, the absorption onset and in particular its composition dependence is similar to independent-particle results. Moreover, classical depolarization effects are responsible for a very strong suppression of the absorption intensity. We show that they can be taken into account in a simpler way using Maxwell-Garnett classical effective-medium theory. Emission spectra are investigated by calculating the absorption of excited nanocrystals at their relaxed geometry. The structural contribution to the Stokes shift is about 0.5 eV. The decomposition of the emission spectra in terms of independent-particle transitions is similar to what is found for absorption. For the emission, very weak transitions are found in Ge-rich clusters well below the strong absorption onset.

PACS numbers: 71.15.Mb, 78.67.-n, 78.67.Bf

I. INTRODUCTION

The semiconductors silicon and germanium can form a substitutional solid solution of the form $\text{Ge}_{1-x}\text{Si}_x$ covering the whole range of compositions x . Pure Si is the most widely used material for electronic applications since many years and its fabrication technology is highly developed. However, the indirect band gap of bulk Si presents a problem for light-emitting applications. A solution that has been proposed to circumvent this problem is nanostructurization of Si in structures comprising porous Si,¹ nanowires,² as well as Si nanocrystals. Moreover, ample use has been made of the fact that Ge can easily be combined with Si in heterostructures. In addition, Ge nanocrystals in a matrix of SiO_2 , SiC, sapphire, or Si have been investigated by many groups.^{3,4,5} In many of those cases, intermixing between Ge and Si is found in the nanostructures.

The two materials show different properties upon nanostructurization. While Si retains its character of an indirect material,^{6,7,8} the work of several groups showed that, depending on the structure, strain, etc., Ge nanostructures can become quasi-direct, i.e., they exhibit very strong transitions at or very close to the HOMO-LUMO transition.^{6,7,8,9,10,11,12} The different behavior reflects the different character of the band gaps in the bulk materials. While both are indirect, the minimum gap in Si lies between Γ and a point near the X point, and the direct gap is much larger. In Ge, the minimum gap between Γ and L is energetically very close to the direct gap at Γ . The effects of confinement and structural relaxation result in a strong contribution of the Γ - Γ transition to

the HOMO-LUMO transition, thus resulting in short radiative lifetimes of Ge clusters.^{8,13}

Therefore, when mixing both materials two questions arise: what is the effect of the intermixing on the electronic properties of the nanocrystals, and how are the different characters of the two materials combined. While the answer to these questions is essentially well known for the bulk alloy, there are still few investigations concerning the mixed nanostructures. Most experimental studies use Stranski-Krastanov growth, (see, e.g., Ref. 14), which results in relatively large structures in which it is safe to assume that the effects of confinement and alloying act independently. However, for smaller structures this cannot be taken for granted. For small nanocrystals, photoluminescence experiments¹⁵ have been compared with theoretical results.¹⁶ Furthermore, Ge-Si nanowires have been investigated experimentally¹⁷ and theoretically.¹⁸

Previous theoretical studies have focused on the interplay of confinement and alloying.^{16,18} However, these *ab initio* calculations were performed within the independent-particle approximation based on the Kohn-Sham scheme of *static* density-functional theory (DFT). Therefore, important many-body effects have been neglected, viz., the self-energy corrections describing the effect of the excitation of the electrons or holes individually, as well as the electron-hole interaction. (Nonetheless, these two effects are found to cancel each other to a large extent for many systems.¹⁹) Furthermore, these calculations miss the very important depolarization or crystal local-field effects.

The way we choose to improve upon the independent-particle results is provided by time-dependent

DFT^{20,21,22} (TDDFT) in which the many-body effects neglected in static DFT are introduced by the so-called exchange-correlation kernel f_{xc} . With respect to the independent-particle results, the excitation energies are corrected, and the transitions between the independent-particle states are mixed. The degree of the mixing indicates the degree to which the independent-particle approximation fails to provide a good description of the system.

Within TDDFT, we use the adiabatic local-density approximation (ALDA, also known as TDLDA) of the exchange-correlation kernel. The choice is motivated by the fact that TDLDA yields good results for optical spectra of isolated systems²³ as well as for non-zero momentum transfers.²⁴ Note, however, that the ALDA is well known to fail in some cases, the most important of which are perhaps extended systems.^{22,25} Within TDDFT, the random-phase approximation (RPA) is obtained by neglecting the exchange-correlation kernel, i.e., by setting $f_{xc} = 0$. From this, the independent-particle approximation results from the neglect of the microscopic terms of the variation of the Hartree potential. In other words, the difference between the independent-particle approximation and the RPA are the depolarization effects which are due to the inhomogeneity of the system.

The simplest way to account for depolarization effects within an approximated classical picture is to apply the Maxwell-Garnett effective-medium theory to the complex dielectric function of the bulk alloy crystals. We applied the effective medium theory to our alloy clusters in order to check if the depolarization effects are dominant with respect to confinement effects and further many-body corrections. In fact, if it is the case, the spectra obtained using the effective-medium theory are in good agreement with full TDLDA results. These model calculations thus give a good overall description of the optical spectra at a much lower computational cost than TDLDA.

In the present paper we first present TDLDA results for $\text{Ge}_{1-x}\text{Si}_x$ nanocrystals, focusing on alloying effects.

The results are then compared with the previous independent-particle calculations of Ref. 16, highlighting the effects of the depolarization, as well as of the mixing of transitions. We will also consider depolarization effects alone, decoupled from confinement effects, by applying Maxwell-Garnett classical effective-medium theory. Finally, the emission properties of the nanocrystals are investigated by considering the geometries obtained after excitation of an electron-hole pair.

II. CALCULATION DETAILS

We used the same modeling scheme as used in Ref. 16 considering $\text{Ge}_{1-x}\text{Si}_x$ nanocrystals with a fixed size made of 83 Ge and Si atoms. Quasi-spherical nanocrystals were built starting from one atom and adding nearest neighbors shell by shell, assuming bulk-like tetrahedral coordination.

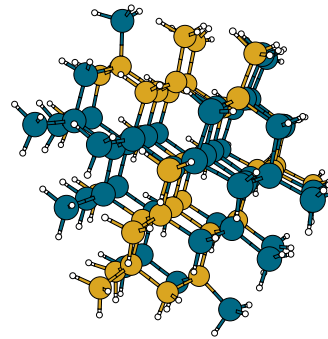


FIG. 1: (Color online) Example of the studied nanocrystal structures: $\text{Ge}_{48}\text{Si}_{35}\text{H}_{108}$. The colors are: Si (yellow), Ge (blue), and H (white).

The outer bonds were saturated by hydrogen atoms. Alloying between Ge and Si was introduced by randomly exchanging Ge atoms by Si. The surface was then passivated with H atoms to saturate the remaining dangling bonds.

In Ref. 16, the study of $\text{Ge}_{1-x}\text{Si}_x$ nanocrystals with the same number of atoms for ten different atomic configurations demonstrated that those with nearly uniformly distributed Ge and Si atoms possess the lowest total energies and nearly equal excitation energies. On the other hand, nanocrystals with deliberately clustered Si atoms and, hence, rather different excitation energies give rise to total energies substantially higher than the average. As their probability of occurrence is, consequently, small, the configurational average can be replaced by the study of only one nanocrystal with nearly uniformly distributed Si and Ge atoms for each composition x . We selected nanocrystals with a total number of 83 atoms of Ge and Si, having a diameter of about 1.5 nm. This radius corresponds to a sphere of the volume occupied by 83 atoms in the bulk. These nanocrystals are large enough to exhibit the characteristics of nanocrystals as opposed to much smaller structures which show a molecular-like behavior.^{6,13,26} Moreover, they are small enough to present significant confinement effects on the electronic states. An example of the atomic arrangement is shown in Fig. 1 for $\text{Ge}_{48}\text{Si}_{35}\text{H}_{108}$.

To obtain the relaxed geometries of the $\text{Ge}_{1-x}\text{Si}_x$ nanocrystals, we used the plane-wave code VASP²⁷ within the local-density approximation (LDA) in the parametrization of Perdew and Zunger²⁸ and the projector-augmented wave (PAW) method.²⁹ This computational set-up is the same as the one employed in Ref.16.

Starting from the relaxed geometries we obtained the optical spectra at zero temperature using TDDFT as implemented in the computer code octopus.^{30,31} The electron-ion interaction is described through norm-conserving pseudopotentials³² and the LDA²⁸ is employed in the adiabatic approximation for the xc potential (i.e., we applied the TDLDA). The time-dependent Kohn-Sham equations, in this code, are represented in

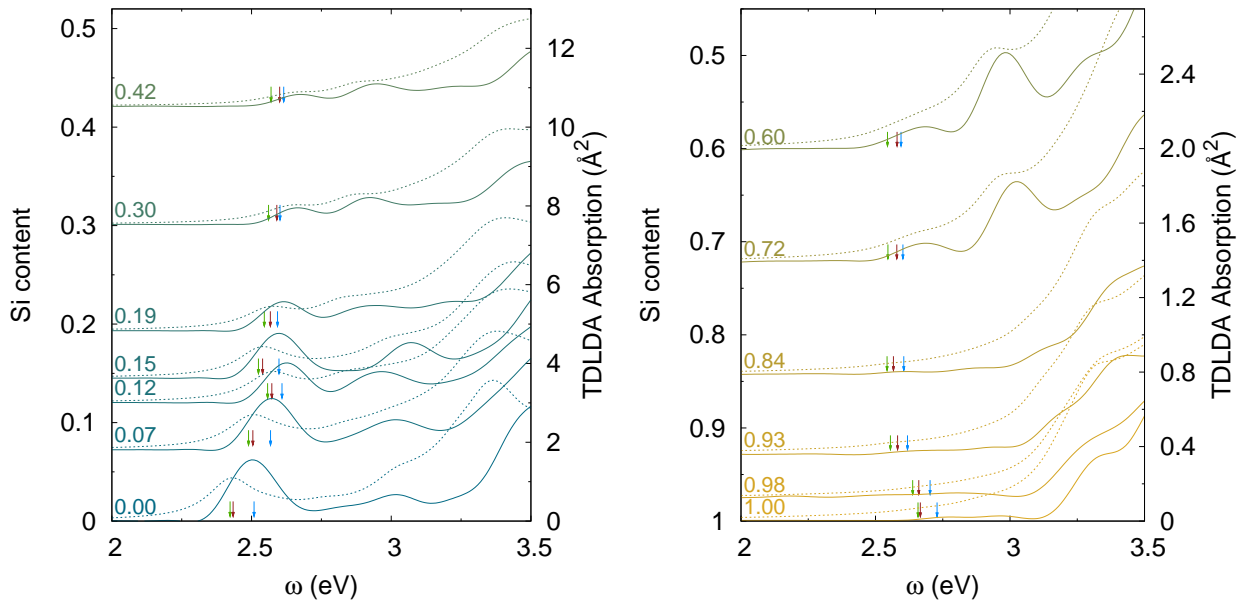


FIG. 2: (Color online) Absorption spectra as a function of the Si content of the clusters: Independent-particle spectra (dashed lines) compared with TDLDA results (solid lines). The green arrows (arrows at lowest energy) mark the HOMO-LUMO gap, while the red arrows (middle arrows) mark the Δ SCF excitation energies and the blue arrows (arrows at highest energy) mark the first transitions of the Casida's analysis. The independent-particle curves are divided by a factor of 15. Note the different scale in the two panels.

a real-space regular grid, using a spacing of 0.275 \AA at which the calculations are converged. The simulation box is constructed by joining spheres of radius 4.5 \AA , centered around each atom.

To calculate the optical response we excite the system from its ground state by applying a delta electric field $E_0\delta(t)$. The real-time response to this perturbation is Fourier transformed to get the dynamical polarizability $\alpha(\omega)$ in the frequency range of interest. The absorption cross section $\sigma(\omega)$, is then obtained from the relation:

$$\sigma(\omega) = \frac{4\pi}{c} \omega \text{Im} \alpha(\omega), \quad (1)$$

where c is the velocity of light in vacuum. For a technical description of this method we refer to Refs. 30 and 33. To obtain the RPA spectra in this approach we just kept the exchange-correlation potential fixed during the propagation (which amounts to making $f_{xc} = 0$). The independent-particle spectra were calculated by further fixing the Hartree potential to its initial value. A time step of $0.0055 \hbar/\text{eV}$ and a total propagation time of $37.5 \hbar/\text{eV}$ were sufficient to ensure a stable propagation. We estimate our numerical precision in the spectra to be better than 0.05 eV . The mixing of independent-particle transitions in the spectra has subsequently been investigated using the Casida's formulation of linear-response TDDFT.^{34,35}

In order to test the coherence of our calculations, we compared independent-particle spectra computed using matrix elements calculated with the VASP code^{6,36,37} to

spectra obtained by time propagation by means of the `octopus` code. No substantial differences were found between the results.

Due to the interest in the luminescence of this kind of systems, the lowest excitation energies are of particular importance. As a consequence, we decided to compare three different quantities. Besides the lowest excitations of the TDLDA absorption spectra, we present the Kohn-Sham HOMO-LUMO gap of the ground state and the Δ SCF excitation energies calculated as the difference $E_{\Delta\text{SCF}} = E(N, e-h) - E(N)$, where $E(N)$ is the total energy of the ground-state and $E(N, e-h)$ is the total energy of the excited-state configuration where one electron has been promoted from the HOMO into the LUMO. In this way, an excited configuration is modeled and the electron-hole interaction is partially taken into account. This approach enables also a subsequent ionic relaxation with the electron-hole pair present, which yields the description of the excited-state geometries. Using the excited-state geometries we were also able to evaluate emission spectra.

III. RESULTS

A. Ground-state geometries: absorption

Results for the photoabsorption of the $\text{Ge}_{1-x}\text{Si}_x$ nanocrystallites are presented in Fig. 2. In the figure we compare the independent-particle response (dashed lines)

with full TDLDA calculations (solid lines) for the whole range of compositions. The dependence of the curves on the composition turns out to be quite smooth. When going from Ge-rich clusters to Si-rich clusters, we observe a shift to higher energies of the onset and a suppression of the absorption strength of the first peak (note the different scales of both panels). Moreover, the dependence of the peak position on the composition x is roughly the same in the independent-particle and the TDLDA schemes. For the clusters studied, the total intensity of the independent-particle spectra is strongly suppressed in TDLDA (the independent particle curves are divided by a factor of 15 in Fig. 2). Indeed, this quenching of the absorption is a well known effect that is due to the inclusion of classical depolarization effects, and not from the exchange-correlation effects accounted for by the TDLDA kernel. This can be verified by calculating the absorption spectrum within the RPA, which includes all classical effects due to the variations of the Hartree potential but neglects quasi-particle and excitonic effects. Indeed, the spectra we calculated within RPA are so close to the TDLDA spectra shown in Fig. 2 that we chose not to show them.

B. Transition analysis and excitation energies

For Ge-rich nanoparticles, both the position and the composition dependence of the peaks are already well described at the level of the independent-particle approximation. This perhaps surprising fact can be explained in terms of compensation of quasiparticle corrections and binding energies of the excitons. For small x at the absorption edge, the first peak is strong and appears essentially at the HOMO-LUMO energy gap. The absorption edge has a completely different nature in Si-rich clusters. In fact, in this case the peaks of lowest energy have a vanishing oscillator strength in TDLDA, thereby blue-shifting the absorption edge with respect to the HOMO-LUMO gap.

In order to analyze the origin of the different peaks in the spectra as a function of the composition of the $\text{Ge}_{1-x}\text{Si}_x$ alloy, we decomposed the excitations in sums of Kohn-Sham particle-hole transitions through the solution of Casida's equation.^{34,35} We found that on the Ge side of the composition range, the lowest peak of the spectra which defines the absorption edge is produced essentially by a strong, pure transition between the Kohn-Sham HOMO and LUMO. This is certainly one more reason for the similarity between the independent-particle and the TDLDA spectra. The large peak with HOMO-LUMO character decreases in intensity with increasing percentage of Si in the $\text{Ge}_{1-x}\text{Si}_x$ alloy, until the composition of about $x = 0.2$ when it disappears. For even smaller x the absorption at the onset is determined by a strong mixture of transitions between states close to HOMO and LUMO. However, the very lowest transitions are forbidden, producing a significant blue shift of

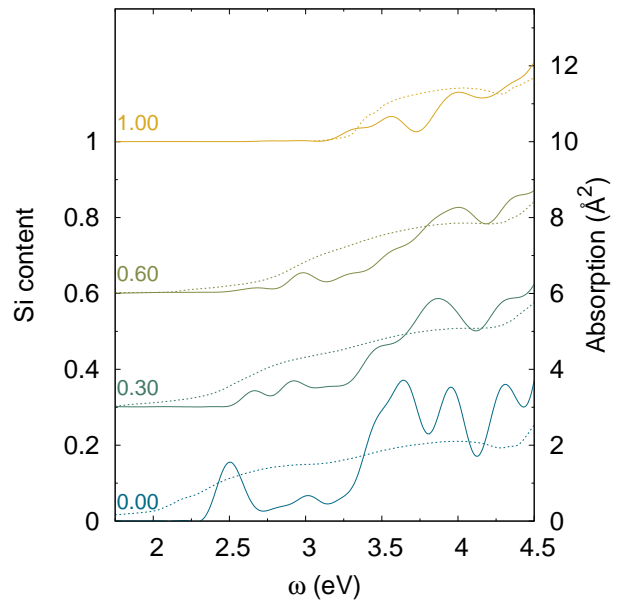


FIG. 3: (Color online) Absorption spectra as a function of the Si content of the clusters: Effective-medium theory (dashed lines) using the dielectric function of bulk $\text{Ge}_{1-x}\text{Si}_x$, compared with TDLDA results (solid lines).

the absorption edge. In the intermediate energy range and for all compositions, excitations can be decomposed as a sum of many contributions.

In Fig. 2 we also show the HOMO-LUMO gap (green arrows), the lowest excitation calculated within the ΔSCF approximation (red arrows), and the first excitation within TDLDA (blue arrows, these excitations are dark on the Si side of the composition). For all cases we find that the first ΔSCF excitation is, as expected, blue-shifted with respect to the HOMO-LUMO gap, and that the first TDLDA transition is at slightly higher energies. The differences are, however, quite small, and of the order of one tenth of an eV. This is known for this class of systems,³⁸ part of it being due to the cancellation of self-energy and excitonic effects.¹⁹ However, the differences appear to be slightly larger in the region of intermediate composition x , i.e., of a greater degree of structural disorder. Similarly, Degoli *et al.* found in Si nanocrystals that the differences become larger in cases of stronger localization.³⁸ It is also clear from the plot how the first transition becomes forbidden while going from Ge-rich to Si-rich clusters — this behavior is reminiscent of the different character of the band gap in the parent bulk Ge and Si.

C. Absorption from classical effective-medium theory

A much simpler approach to model the absorption cross section of a $\text{Ge}_{1-x}\text{Si}_x$ nanocrystal is to start from

the complex dielectric function of the corresponding bulk alloy crystal and to apply the effective-medium theory.^{39,40} This classical approach is based on Maxwell's equations and neglects completely the microscopic details, such as atoms and bonds. Of course, this assumption is better justified when the size of the system is large. However, it always handles correctly the boundary conditions for the Maxwell's equations at the interfaces, which give the very important contributions to the dielectric response through the classical depolarization effects. Often, these classical contributions are enough to describe the physics of the dielectric response of a composite system made of objects embedded in some matrix.^{41,42,43} Our clusters can be considered as a family of spheres of volume V_{obj} cut from a $\text{Ge}_{1-x}\text{Si}_x$ bulk alloy. The Maxwell-Garnett expression³⁹ in the specific case of an isolated spherical object in vacuum yields:

$$\sigma(\omega) = 9\frac{\omega}{c}V_{\text{obj}}\frac{\Im\epsilon(\omega)}{[\Re\epsilon(\omega) + 2]^2 + [\Im\epsilon(\omega)]^2}, \quad (2)$$

where ϵ is the experimental complex dielectric function of the bulk alloy. To represent well the extension of the polarizable nanocrystals, we took an average distance of the furthest saturating hydrogen atoms to obtain the radius of the cluster, and consequently V_{obj} . This results in a radius slightly larger than the one mentioned above which takes into account only the Ge and Si atoms. We used the value of $R_{\text{obj}} = 9.1 \text{ \AA}$, but the results are fairly insensitive to a (reasonable) choice of this value. The experimental dielectric function of the bulk alloy with precisely the needed composition x has been obtained from a discrete set of measurements⁴⁴ using a recently developed interpolation scheme.⁴⁵ This scheme interpolates $\Im\epsilon(\omega)$ making use of the screening sum rule and the positive definiteness of the spectra. $\Re\epsilon(\omega)$ was subsequently obtained by means of the Kramers-Kronig relations after fitting appropriate tails to the imaginary parts. The latter procedure was tested on the input curves to insure the quality of the real part.

In Fig. 3 we show spectra calculated using the effective-medium theory for selected compositions. Comparing to the first-principles TDLDA curves, we can see that, already for this relatively small size of clusters, the classical theory gives a quite good overall description of the absorption spectrum. As expected, effective-medium theory is not capable of describing the peaks of the individual transitions, but it describes correctly the intensity and the trends of the spectrum. Once again these results confirm that the dependence on the composition of the optical spectra is smooth and that the confinement and alloying effects act independent to a large degree. In fact, within this classical scheme, only the alloying effects determine the variation of the absorption response as a function of x . In particular, the confinement-induced opening of the HOMO-LUMO gaps and the resulting blue-shift of the absorption onset are not accounted for. The confinement effects could be described by introducing a size-dependent crystallite dielectric function which

can then be used to calculate the spectra of the crystallites in a different environment.²⁶ In this sense, comparison of the TDLDA results with the present effective-medium approach gives an idea of the importance of the confinement effects on the overall spectra.

We note that these model calculations can be performed at negligible computational cost, and therefore provide a simple and fast method to obtain reasonable spectra for medium and large nanocrystallites.

Given the strong influence of the depolarization effects, the question arises as to why the independent-particle spectra have been successfully compared previously with experiment.⁶ This agreement is, in fact, not a fortuitous coincidence, but due to the experimental conditions. The experiment has been done on Ge NCs inside a matrix of sapphire.⁴⁶ This reduces strongly the depolarization effects because it reduces the inhomogeneity of the system. The calculations, on the other hand, treated NCs in vacuum but neglected the depolarization effects. Therefore, together with the cancellation between self-energy effects and electron-hole interaction mentioned above, the independent-particle approximation provides in fact a good description of the spectra of this particular experiment.

D. Excited-state geometries: emission

In order to calculate the emission properties, we consider the geometry of the relaxed nanocrystals where the ionic relaxation has been carried out after transferring an electron from the HOMO to the LUMO Kohn-Sham orbital. As the radiative lifetimes are usually much longer than the times that the electrons (holes) take to relax to the LUMO (HOMO), we can assume thermalized electron-hole pairs. As their lifetimes are then determined by the exponential factor describing their distribution,^{47,48} it is the onset of the emission which reflects the emission properties, while the higher parts of the spectrum are suppressed.

Stimulated emission spectra can be easily obtained within our formalism by calculating the absorption cross-section $\tilde{\sigma}_{\text{abs}}(\omega)$ at the excited-state geometry. Luminescence spectra can then be calculated from the van Roosbroeck-Shockley model⁴⁹

$$\sigma_{\text{lum}}(\omega) \sim \omega^2 \frac{1}{e^{\hbar\omega/k_b T} - 1} \tilde{\sigma}_{\text{abs}}(\omega), \quad (3)$$

where k_b is the Boltzmann constant and T is the temperature.

In Fig. 4 we compare the absorption cross sections for the ground-state (solid lines) and the excited-state (dashed lines) geometries for $\text{Ge}_{1-x}\text{Si}_x$ clusters in all the composition range. The energy difference between the onsets of absorption and emission corresponds to the structural contribution to the Stokes shift.

In Fig. 5 we compare the independent-particle result with the TDLDA for the absorption $\tilde{\sigma}_{\text{abs}}(\omega)$ at the

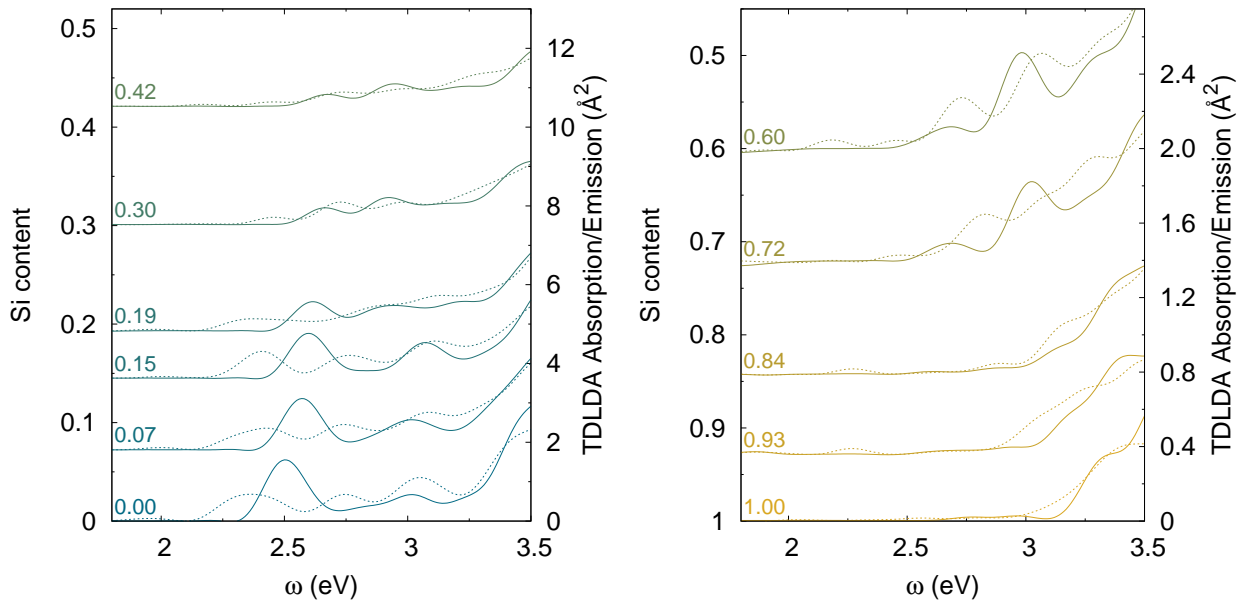


FIG. 4: (Color online) Absorption (solid lines) and emission (dashed lines) spectra as a function of the Si content of the clusters. Note the different scales.

excited-state geometry. The conclusions with respect to their similarity drawn for the ground state remain valid for the excited-state geometries. The same applies to the transition analysis using Casida's equation. The character of the emission onset on the Ge side of the composition range is already well described within the independent-particle approximation. The decomposition of the excitations as a sum of Kohn-Sham transitions provides a picture strictly analogous to the one for the absorption spectra: the lowest transitions of the Ge-rich nanocrystals correspond to almost pure Kohn-Sham transitions, while for large x and for the higher transitions, independently of x , strong mixing is found.

However, it is important to note that a very weak peak appears at about 1.95 eV. This is red-shifted by about 0.5 eV with respect to the ground-state calculation. The peak, which can be easily seen in Fig. 5, is clearly present in both the independent-particle result and the TDLDA result. It occurs for all compositions on the Ge side of the x range and is almost composition independent. It appears to be connected with the lowering of the symmetry as compared to the ground state where the pure Si or Ge nanocrystals without alloying have T_d symmetry and the HOMO-LUMO transition is threefold degenerate. The symmetry breaking due to the geometry relaxation under excitation has therefore a much stronger effect than the introduction of the alloying, which at the Ge-rich side splits the degeneracy only slightly and which does not change the character of the strong absorption onset at the HOMO-LUMO transition. Due to the argument above, cf. Eq. 3, the appearance of this weak peak will strongly increase the radiative lifetimes of the systems. We conjecture that this might be responsible for the fact

that even though several theoretical predictions coincide in that Ge nanostructures should have strong transitions at the absorption onset, few experiments have been able to detect luminescence from excitons in Ge nanocrystals.

IV. CONCLUSIONS

The absorption spectra of free $\text{Ge}_{1-x}\text{Si}_x$ have been calculated within time-dependent density-functional theory in the adiabatic local-density approximation. The changes of the spectra upon changing composition x are smooth. In particular at the absorption onset, the position and the composition dependence of the spectra is found to be already well represented by independent-particle results. The analysis of the solutions of Casida's equation show that this is due to the fact that the first transition of Ge-rich nanocrystals corresponds to an almost pure independent-particle transition. The TDLDA onsets are slightly blue-shifted with respect to their independent-particle counterpart, their composition dependence at the Ge side of the compositional range is practically the same. For higher Si contents, a mixing of many independent-particle transitions is found.

Depolarization effects are strong and their inclusion alone, even within a simplified classical model, on top of an independent-particle calculation allows to get the correct physical picture of the optical response. They can be approximately taken into account at a negligible computational cost using Maxwell-Garnett effective-medium theory.

Further many-body terms do not modify significantly the spectra due to the cancellation of opposite contri-

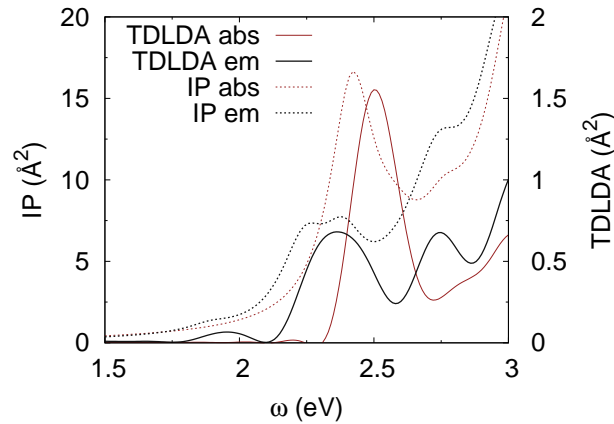


FIG. 5: (Color online) Absorption (red) and emission (black) spectra of the pure Ge nanocrystal in the independent-particle approximation (dashed) and the TDLDA (solid). Note the different scales.

contributions given by quasiparticle corrections and excitonic effects. As a consequence, the effects of the excitation of an electron-hole pair do not alter the comparison between the independent-particle spectra and the TDLDA results.

Emission spectra have been investigated using the geometry of excited nanocrystals. A Stokes shift of about 0.5 eV is found. Very weak peaks appear at the absorption onset for all systems on the Ge side which suppress the radiative transition probability and lead to long radiative lifetimes.

V. ACKNOWLEDGMENTS

The authors would like to thank Lucia Reining for many fruitful discussions. All TDDFT calculations

were performed at the Laboratório de Computação Avançada of the University of Coimbra. The authors were partially supported by the EC Network of Excellence NANOQUANTA (NMP4-CT-2004-500198) and the ETSF e-I3 (INFRA-2007-211956). S. Botti acknowledges financial support from French ANR (JC05_46741 and NT05-3_43900). H.-Ch. W. acknowledges support from the European Union through the individual Marie Curie Intra-European Grant No. MEIF-CT-2005-025067. M. A. L. Marques acknowledges partial support from the Portuguese FCT through the project PTDC/FIS/73578/2006 and from the French ANR (ANR-08-CEXC8-008-01).

-
- ¹ O. Bisi, S. Ossicini, and L. Pavesi, *Surf. Sci. Rep.* **38**, 1 (2000).
 - ² W. Lu and C. M. Lieber, *J. Physics D: Appl. Phys.* **39**, R387 (2006).
 - ³ S. Takeoka, M. Fujii, S. Hayashi, and K. Yamamoto, *Phys. Rev. B* **58**, 7921 (1998).
 - ⁴ J. P. Wilcoxon, P. P. Provencio, and G. A. Samara, *Phys. Rev. B* **64**, 035417 (2001).
 - ⁵ C. Schubert, U. Kaiser, A. Hedler, W. Wesch, T. Gorelik, U. Glatzel, J. K. Ilich, B. Wunderlich, G. Heß, and K. Goetz, *J. Appl. Phys.* **91**, 1520 (2002).
 - ⁶ H.-Ch. Weissker, J. Furthmüller, and F. Bechstedt, *Phys. Rev. B* **65**, 155328 (2002).
 - ⁷ H.-Ch. Weissker, J. Furthmüller, and F. Bechstedt, *Phys. Rev. B* **67**, 245304 (2003).
 - ⁸ H.-Ch. Weissker, J. Furthmüller, and F. Bechstedt, *Mat. Sci. Eng. B* **101**, 39 (2003).
 - ⁹ A. N. Kholod, S. Ossicini, V. E. Borisenko, and F. Arnaud d'Avitaya, *Phys. Rev. B* **65**, 115315 (2002).
 - ¹⁰ A. N. Kholod, V. L. Shaposhnikov, N. Sobolev, V. E. Borisenko, F. A. D'Avitaya, and S. Ossicini, *Phys. Rev. B* **70**, 035317 (2004).
 - ¹¹ A. Tzolakis and R. M. Martin, *Phys. Rev. B* **71**, 125319 (2005).
 - ¹² D. Melnikov and J. Chelikowsky, *Solid State Commun.* **127**, 361 (2003).
 - ¹³ H.-Ch. Weissker, J. Furthmüller, and F. Bechstedt, *Phys. Rev. B* **69**, 115310 (2004).
 - ¹⁴ O. G. Schmidt, U. Denker, S. Christiansen, and F. Ernst, *Appl. Phys. Lett.* **81**, 2614 (2002).
 - ¹⁵ S. Takeoka, K. Toshikiyo, M. Fujii, S. Hayashi, and K. Yamamoto, *Phys. Rev. B* **61**, 15988 (2000).
 - ¹⁶ H.-Ch. Weissker, J. Furthmüller, and F. Bechstedt, *Phys. Rev. Lett.* **90**, 085501 (2003).
 - ¹⁷ J.-E. Yang, C.-B. Jin, C.-J. Kim, and M.-H. Jo, *Nano Letters* **6**, 2679 (2006).
 - ¹⁸ D. B. Migas and V. E. Borisenko, *Phys. Rev. B* **76**, 035440 (2007).
 - ¹⁹ C. Delerue, M. Lannoo, and G. Allan, *Phys. Rev. Lett.* **84**, 2457 (2000).

- ²⁰ E. Runge and E. Gross, Phys. Rev. Lett. **52**, 997 (1984).
- ²¹ M. A. L. Marques, C. Ullrich, F. Nogueira, A. Rubio, K. Burke, and E. K. U. Gross, eds., *Time-Dependent Density Functional Theory*, vol. 706 of *Lecture Notes in Physics* (Springer-Verlag, Berlin, 2006).
- ²² S. Botti, A. Schindlmayr, R. Del Sole, and L. Reining, Rep. Prog. Phys. **70**, 357 (2007).
- ²³ M. A. L. Marques, A. Castro, and A. Rubio, J. Chem. Phys. **115**, 3006 (2001).
- ²⁴ H.-Ch. Weissker, J. Serrano, S. Huotari, F. Bruneval, F. Sottile, G. Monaco, M. Krisch, V. Olevano, and L. Reining, Phys. Rev. Lett. **97**, 237602 (2006).
- ²⁵ G. Onida, L. Reining, and A. Rubio, Rev. Mod. Phys. **74**, 601 (2002), and references therein.
- ²⁶ H.-Ch. Weissker, J. Furthmüller, and F. Bechstedt, Phys. Rev. B **67**, 165322 (2003).
- ²⁷ <http://cms.mpi.univie.ac.at/vasp/>.
- ²⁸ J. P. Perdew and A. Zunger, Phys. Rev. B **23**, 5048 (1981).
- ²⁹ P. E. Blöchl, Phys. Rev. B **50**, 17953 (1994).
- ³⁰ M. A. L. Marques, A. Castro, G. F. Bertsch, and A. Rubio, Comp. Phys. Comm. **151**, 60 (2003).
- ³¹ A. Castro, M. A. L. Marques, H. Appel, M. Oliveira, C. Rozzi, X. Andrade, F. Lorenzen, E. K. U. Gross, and A. Rubio, Phys. Stat. Sol. (b) **243**, 2465 (2006).
- ³² N. Troullier and J. Martins, Phys. Rev. B **43**, 1993 (1991).
- ³³ A. Castro, M. A. L. Marques, J. A. Alonso, and A. Rubio, J. Comp. Theoret. Nanoscience **1**, 231 (2004).
- ³⁴ M. E. Casida, in *Recent Advances in Density Functional Methods*, Part I, edited by D. Chong (World Scientific, 1995), p. 155.
- ³⁵ M. E. Casida, in *Recent Developments and Applications of Modern Density Functional Theory*, edited by J. Seminario (Elsevier Science, Amsterdam, 1996), p. 391.
- ³⁶ B. Adolph, J. Furthmüller, and F. Bechstedt, Phys. Rev. B **63**, 125108 (2001).
- ³⁷ H.-Ch. Weissker, J. Furthmüller, and F. Bechstedt, Phys. Rev. B **64**, 035105 (2001).
- ³⁸ E. Degoli, G. Cantele, E. Luppi, R. Magri, D. Ninno, O. Bisi, and S. Ossicini, Phys. Rev. B **69**, 155411 (2004).
- ³⁹ J. Maxwell-Garnett, Philos. Trans. R. Soc. **203**, 305 (1904).
- ⁴⁰ D. M. Wood and N. W. Ashcroft, Philos. Mag. **35**, 269 (1977).
- ⁴¹ F. Sottile, F. Bruneval, A. G. Marinopoulos, L. K. Dash, S. Botti, V. Olevano, N. Vast, A. Rubio, and L. Reining, Int. J. Quantum Chem. **102**, 684 (2005).
- ⁴² S. Botti, N. V. V. Olevano, L. Reining, and L. C. Andreani, Phys. Rev. Lett. **89**, 216803 (2002).
- ⁴³ S. Botti, N. V. V. Olevano, L. Reining, and L. C. Andreani, Phys. Rev. B **70**, 045301 (2004).
- ⁴⁴ J. Humlíček, M. Garriga, M. I. Alonso, and M. Cardona, J. Appl. Phys. **65**, 2827 (1989).
- ⁴⁵ H.-Ch. Weissker, V. Olevano, and L. Reining, Phys. Rev. B, in press (2009).
- ⁴⁶ P. Tognini, L. C. Andreani, M. Geddo, A. Stella, P. Cheyssac, R. Kofman, and A. Migliori, Phys. Rev. B **53**, 6992 (1996).
- ⁴⁷ D. Dexter, Solid State Physics – Advances in Research and Applications **6**, 353 (1958).
- ⁴⁸ C. Delerue, G. Allan, and M. Lannoo, Phys. Rev. B **48**, 11024 (1993).
- ⁴⁹ W. van Roosbroeck and W. Shockley, Phys. Rev. **94**, 1558 (1954).